THE JOURNAL OF BIOLOGICAL CHEMISTRY VOL. 280, NO. 51, pp. 42172–42180, December 23, 2005

Nitrosylation of Human Glutathione Transferase P1-1 with Dinitrosyl Diglutathionyl Iron Complex *in Vitro* and *in Vivo*[*]

Received for publication, July 20, 2005, and in revised form, September 15, 2005 Published, JBC Papers in Press, September 29, 2005, DOI 10.1074/jbc.M507916200

Eleonora Cesareo[‡1], Lorien J. Parker[§1,2], Jens Z. Pedersen[‡], Marzia Nuccetelli[¶], Anna P. Mazzetti[‡], Anna Pastore[‖], Giorgio Federici[¶‖], Anna M. Caccuri[**], Giorgio Ricci[**], Julian J. Adams[§], Michael W. Parker[§3], and Mario Lo Bello[‡4]

From the Departments of [‡]Biology, [**]Chemical Sciences, and Technologies, and [¶]Internal Medicine, University of Rome "Tor Vergata," 00133 Rome, Italy, [§]Biota Structural Biology Laboratory, St. Vincent's Institute of Medical Research, 9 Princes Street, Fitzroy, Victoria 3065, Australia, and [‖]The Children's Hospital IRCCS "Bambino Gesù," 00165 Rome, Italy

We have recently shown that dinitrosyl diglutathionyl iron complex, a possible *in vivo* nitric oxide (NO) donor, binds with extraordinary affinity to one of the active sites of human glutathione transferase (GST) P1-1 and triggers negative cooperativity in the neighboring subunit of the dimer. This strong interaction has also been observed in the human Mu, Alpha, and Theta GST classes, suggesting a common mechanism by which GSTs may act as intracellular NO carriers or scavengers. We present here the crystal structure of GST P1-1 in complex with the dinitrosyl diglutathionyl iron ligand at high resolution. In this complex the active site Tyr-7 coordinates to the iron atom through its phenolate group by displacing one of the GSH ligands. The crucial importance of this catalytic residue in binding the nitric oxide donor is demonstrated by site-directed mutagenesis of this residue with His, Cys, or Phe residues. The relative binding affinity for the complex is strongly reduced in all three mutants by about 3 orders of magnitude with respect to the wild type. Electron paramagnetic resonance spectroscopy studies on intact *Escherichia coli* cells expressing the recombinant GST P1-1 enzyme indicate that bacterial cells, in response to NO treatment, are able to form the dinitrosyl diglutathionyl iron complex using intracellular iron and GSH. We hypothesize the complex is stabilized *in vivo* through binding to GST P1-1.

S-Nitrosylation of protein thiol groups by nitric oxide is accepted as being among the most important posttranslational modifications (1). Such modifications can cause modulation of many different functions with recent examples including proteins involved in signaling cascades, apoptosis, ion channels, redox systems, and hemoproteins (2). It has been suggested that NO may play a role in iron homeostasis and/or metabolism based on observations of iron nitrosylation of non-heme iron proteins in bacteria (3) as well as in mammals (4–6). Iron-free proteins, such as albumin (7) and GSH reductase (8), can also become targets of nitrosylation in the presence of suitable amounts of iron and thiol ligand (mostly GSH under physiological conditions). In these cases the formation of iron-dithiol dinitrosyl complexes are readily detected by EPR spectroscopy. We have recently shown that human glutathione transferase (GST)[5] P1-1 strongly binds dinitrosyl diglutathionyl iron complexes (DNDGIC) *in vitro* while maintaining its well known detoxifying activity toward dangerous compounds (9). A very high affinity for this complex was also found for other glutathione transferase classes (Mu, Alpha, and Theta), suggesting a common mechanism by which the more recently evolved GSTs may act as intracellular NO carriers or scavengers (10, 11).

The glutathione transferases (EC 2.5.1.18), historically also called glutathione *S*-transferases, catalyze the nucleophilic attack by reduced glutathione (GSH) on non-polar compounds that contain an electrophilic carbon, nitrogen, or sulfur atom. This classical conjugation reaction toward foreign compounds (*e.g.* cancer chemotherapeutic agents, insecticides, herbicides, carcinogens) and endogenous compounds (*e.g.* byproducts of oxidative stress) is considered part of a coordinated defense strategy together with other GSH-dependent enzymes, the cytochrome P450s (Phase I enzymes) and some membrane transporters (Phase III) such as MRP1 and MRP2, to remove glutathione conjugates from the cell. In mammals there are three major families of proteins widely distributed in nature that exhibit glutathione transferase activity. Two of these, the cytosolic and mitochondrial GSTs, comprise soluble enzymes, whereas the third family is microsomal and is referred to as MAPEG (membrane-associated proteins in eicosanoid and glutathione) metabolism (12). The human cytosolic GSTs are dimeric proteins that can be grouped into at least seven gene-independent classes (Alpha, Mu, Pi, Sigma, Theta, Omega, and Zeta) on the basis of their amino acid sequence and immunological properties (13–16). Their three-dimensional structures do not differ significantly despite low sequence homology (17–20). Each subunit contains a very similar binding site for GSH (G-site) and a second one for the hydrophobic cosubstrate (H-site). Structural differences at the H-site confer a certain degree of substrate selectivity. Despite a common structure they appear to play multiple functions. For example, Zeta class GST Z1–1 is involved in the catabolism of phenylalanine (21), Pi class GST P1-1 and Mu class GST M1–1 are involved in signaling pathways through physical interaction with some kinases (22, 23), and Omega class GST O1–1 modulates calcium channels, thus protecting mammalian cells from apoptosis induced by Ca^{2+} mobilization (24).

In this paper we report the crystallographic structure of GST P1-1

[*] This work was supported in part by the Australian Synchrotron Research Program, which is funded by the Commonwealth of Australia under the Major National Research Facilities Program. Use of the Advanced Photon Source was supported by the United States Department of Energy, Basic Energy Sciences, Office of Energy Research. This work was also supported by a grant from the Australian Research Council (to M. W. P.). The costs of publication of this article were defrayed in part by the payment of page charges. This article must therefore be hereby marked "*advertisement*" in accordance with 18 U.S.C. Section 1734 solely to indicate this fact.

The atomic coordinates and structure factors (code 1ZGN) have been deposited in the Protein Data Bank, Research Collaboratory for Structural Bioinformatics, Rutgers University, New Brunswick, NJ (http://www.rcsb.org/).

[1] These authors contributed equally to this work.

[2] Supported by a National Health and Medical Research Council of Australia Dora Lush Scholarship.

[3] A National Health and Medical Research Council of Australia Fellow.

[4] Supported in part by Ministero dell'Università e della Ricerca Scientifica e Tecnologica Italy (COFIN 2004). To whom correspondence should be addressed. Tel.: 390-6-72594375; Fax: 390-6-2025450; E-mail: lobello@uniroma2.it.

[5] The abbreviations used are: GST, glutathione transferase; CDNB, 1-chloro-2,4-dinitrobenzene; NONOate, 2-(*N*,*N*-diethylamino)-diazenolate 2-oxide; DEANO, diethylamine NONOate; DNDGIC, dinitrosyl diglutathionyl iron complex; DNGIC, dinitrosyl glutathionyl iron complex; MES, 2-(*N*-morpholino)ethanesulfonic acid; WT, wild-type enzyme; GSNO, *S*-nitrosoglutathione.

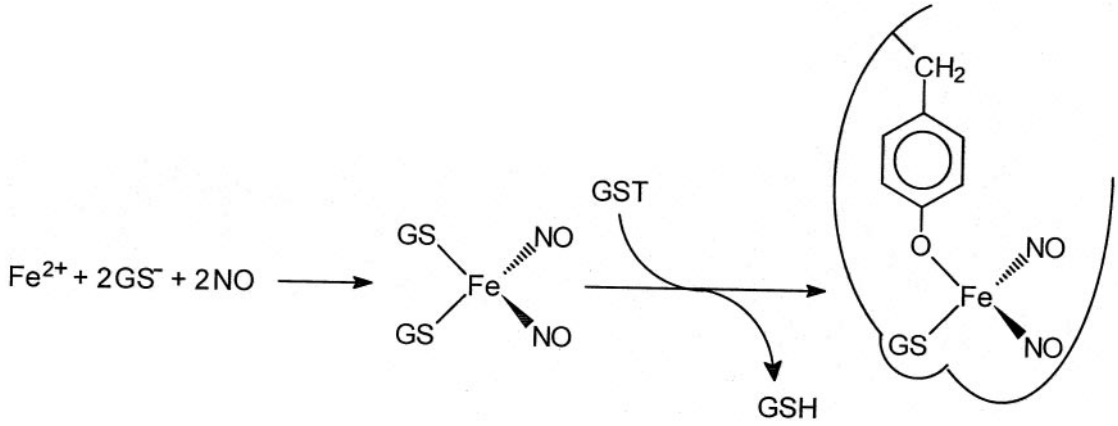

SCHEME 1

with the DNDGIC bound in the active site, which together with site-directed mutagenesis studies demonstrate a crucial role for the catalytic residue Tyr-7 acting as a ligand for the iron complex in the active site (Scheme 1). These data provide direct support that GSTs can be nitrosylated *in vitro*. Further studies on intact *Escherichia coli* cells upon exposure to either GSNO or diethylamine NONOate suggest that human GST P1-1 can also be nitrosylated inside the cell.

EXPERIMENTAL PROCEDURES

Chemicals—Diethylamine NONOate (DEANO) was from Calbiochem. GSH, 1-chloro-2,4-dinitrobenzene (CDNB), and other reagents used were from Sigma. DEANO solutions were prepared in phosphate-buffered saline buffer, pH 7.4, at room temperature; under these conditions the half-life of NO release is 16 min.

GSNO Synthesis—GSNO was prepared by a modification of the original published procedure (9, 27, 28). 3 ml of equimolar GSH and $NaNO_2$ (33 mM) were vortexed and placed on ice for an hour. To this solution 45 μl of 11 M HCl was added and vortexed, and the solution was again placed on ice for a further 2 h. 40 μl of 10 M NaOH was then added to neutralize the solution. 4 ml of acetone were added, and the GSNO sank to the bottom of the tube as a pink oil. The upper layer of acetone/H_2O was aspirated off. GSNO was re-suspended in 500 μl of H_2O, and again 4 ml of acetone was added. The solution was mixed and then left to sit for an hour until the GSNO oil sank to the bottom. The upper solution was again aspirated away. The resulting pink oil was frozen to −196 °C and placed on a freeze dryer for 4 h. The resulting pink solid (yield of ~0.89 mmol) had a UV spectrum consistent with published reports (27, 29). The compound was wrapped in aluminum foil to exclude light and stored at 4 °C. The GSNO concentration was determined by UV-visible spectroscopy as described (9); the purity was comparable with that of commercially available GSNO.

Dinitrosyl Diglutathionyl Iron Complex Synthesis—DNDGIC was prepared by a modification of the original published procedure (9). To 50 μl of 100 mM MES buffer, pH 6.0, and 200 μl of 100 mM GSH, 20 μl of 100 mM GSNO was added. Finally, 2 μl of 1 M $FeSO_4$ solution containing 0.5 mM vitamin C was added. The final concentrations were 40 mM GSH, 4 mM GSNO, 4 mM $FeSO_4$, and 1 μM vitamin C in a 500-μl volume. After several hours on ice wrapped in aluminum foil to exclude light, the solution turned a strong yellow color that was stable, contrary to previous reports, for up to a week (9–11). UV spectra were consistent with previous reports (9–11). DNDGIC cannot be isolated as a solid due to dimerization (30) but is stabilized in solution by the large excess of GSH present.

Crystallization—Wild-type human Pi class GST P1-1 was expressed and purified as previously described (25). The protein was crystallized using the hanging drop vapor diffusion method as described elsewhere (26). Briefly, a 2-μl drop of protein (concentration of 6.7 mg/ml in 1 mM EDTA, 1 mM mercaptoethanol, and 10 mM phosphate buffer, pH 7.0) was mixed with the same volume of reservoir buffer composed of 100 mM MES buffer, pH 5.5 or 6.0, 22% (w/v) polyethylene glycol 8000, 20 mM $CaCl_2$, 10 mM dithiothreitol, and 10 mM GSH. Crystals grew at 22 °C and reached a suitable size in approximately a week.

Dinitrosyl Diglutathionyl Iron Complex Soak—Wild-type crystals were transferred into a new drop containing 200 μl of the DNDGIC solution described above, 100 mM MES buffer, pH 6.0, 22% (w/v) polyethylene glycol 8000, and 20 mM $CaCl_2$. These crystals were soaked for several days.

Data Collection and Processing—The x-ray diffraction data were collected at the Advanced Photon Source (Chicago, Illinois), beam line 14-ID-B using a MAR165 CCD MARResearch detector. The wavelength was set to 0.99 Å. For cryoprotection the crystals were soaked for 2 min in the well solution containing 5% (v/v) methyl-2,4-pentanediol (MPD), then dipped briefly in well solution containing 10% (v/v) MPD. The crystals were then snap-frozen at 100 K in the cryostream. Diffraction data were processed and scaled with HKL (31). The crystals were shown to belong to a monoclinic lattice, with the space group C2, as seen previously for the wild-type GST P1-1 (26).

Structure Determination and Refinement—Refinement began with the Pi class GST in the C2 space group (5GSS (26)) that had GSH and water molecules removed. Rigid body refinement in CNS (32) was used to compensate for any possible changes in crystal packing. The starting model gave an *R*-factor of 33.0% (R_{free} = 35.3%). The model was then refined by a round of simulated annealing using CNS. Because the asymmetric unit of the crystal contained two GST monomers, use was made of the non-crystallographic symmetry restraints on all non-hydrogen atoms in the initial rounds of the refinement. The model was rebuilt with TURBO (33), and GSH, MES, and water molecules were added. The model was further refined with cycles of positional and isotropically restrained B-factor refinement. After several rounds of refinement, the density for the iron complex was evident in a $F_o - F_c$ map and was subsequently built into the model. An absorption scan at the iron edge, at 7.13 keV or 1.74 Å, demonstrated the presence of the metal in the crystal. However, data collected from this crystal were limited to a resolution of 2.7 Å because of radiation damage at this wavelength. Thus, the data were recollected at 0.99 Å off a fresh crystal. After multiple rounds of refinement and rebuilding the final *R*-factor was 18.2% (R_{free} = 24.4%) for all data to 2.1 Å of resolution. The stereochemistry was analyzed with the program PROCHECK (34) and gave values either similar or better than expected for structures refined at similar resolu-

TABLE ONE

Summary of data collection and structure refinement for the DNGIC-GST P1-1 complex

The values in parentheses are for the highest resolution bin.

Data collection	
Temperature (K)	100
Space group	C2
Cell dimensions	
a (Å)	76.2
b (Å)	89.8
c (Å)	68.7
β (°)	97.6
Maximum resolution (Å)	2.1 (2.18-2.10)
No. of crystals	1
No. of observations	2,076,942
No. of unique reflections	24,224 (1,811)
Data completeness (%)	90.1 (68.0)
I/σ	27.1 (8.33)
Multiplicity	85.7 (13.5)
R_{merge} [a] (%)	6.1 (17.1)
Refinement	
Non-hydrogen atoms	
Protein	3,260
DNGIC	50
MES	24
Solvent (H_2O)	242
Resolution (Å)	2.1 (2.18-2.10)
R_{conv} [b] (%)	18.2 (20.7)
R_{free} [c] (%)	24.4 (28.4)
Reflections used in R_{conv} calculations	
Number	22,998 (1729)
Completeness (%)	85.8 (67.9)
Root mean square deviation from ideal geometry	
Bonds (Å)	0.005
Angles (°)	1.2
Mean *B* (protein) (Å^2)	29.2
Main chain	27.7
Side chain	30.8
Iron	43.3
NO	33.1
GSH	31.1
Mean *B* (solvent) (Å^2)	33.0
Residues in most favored regions of Ramachandran plot (%)	92.5
Residues in allowed regions of Ramachandran plot (%)	5.8
Residues in generously allowed regions of Ramachandran plot (%)	1.7
Residues in disallowed regions of Ramachandran plot (%)	0

[a] $R_{merge} = \Sigma_{hkl}\Sigma_i|I_i - \langle I\rangle|/|\langle I\rangle|$, where I_i is the intensity for the *i*th measurement of an equivalent reflection with indices *h*, *k*, and *l*.
[b] $R_{conv} = \Sigma||F_{obs}| - |F_{calc}||/\Sigma|F_{obs}|$, where F_{obs} and F_{calc} are the observed and calculated structure factor amplitudes, respectively.
[c] R_{free} was calculated with 5% of the diffraction data that were selected randomly and not used throughout refinement.

tions. Data collection results and a summary of the refinement statistics are given in TABLE ONE.

Expression Plasmids and Site-directed Mutagenesis—The plasmid pGST-1, producing large amounts of recombinant wild-type GST P1-1 in the cytoplasm of *E. coli*, has been described previously (25). Site-directed mutagenesis of Tyr-7 into Phe, His, and Cys residues was accomplished using the same strategy adopted for the plasmid pGST-1 except that the synthetic linkers with *NcoI-TaqI*-compatible ends were obtained by annealing the following complementary oligonucleotides: 5′-CATGCCACCGTACACCGTTGTT**TTC**TTCCCGGTT and 5′-CGAACCGGGAA**GAA**AACAACGGTGTACGGTGG (Phe-7); 5′-CATGCCACCGTACACCGTTGTT**CAT**TTCCCGGTT and 5′-CGAACCGGGAA**ATG**AACAACGGTGTACGGTGG (His-7); 5′-CATGCCACCGTACACCGTTGTT**TGC**TTCCCGGTT and 5′-CGAACCGGGAA**GCA**AACAACGGTGTACGGTGG (Cys-7).

Protein Expression and Purification—Native and mutant GST P1-1 enzymes were produced as described previously (25, 35). Briefly, *E. coli* strain TOP 10 cells, harboring plasmid pGST-1 or plasmids expressing Phe-7, His-7, or Cys-7 mutant enzymes (pGST-F7, pGST-H7, pGST-C7), were grown in Luria broth containing 100 μg/ml ampicillin and 50 μg/ml streptomycin. The expression of GST was induced by the addition of 0.2 mM isopropyl-1-thio-β-galactopyranoside when the absorbance at 600 nm was 0.5. Eighteen hours after induction cells were harvested by centrifugation and lysed as previously described (25). Native

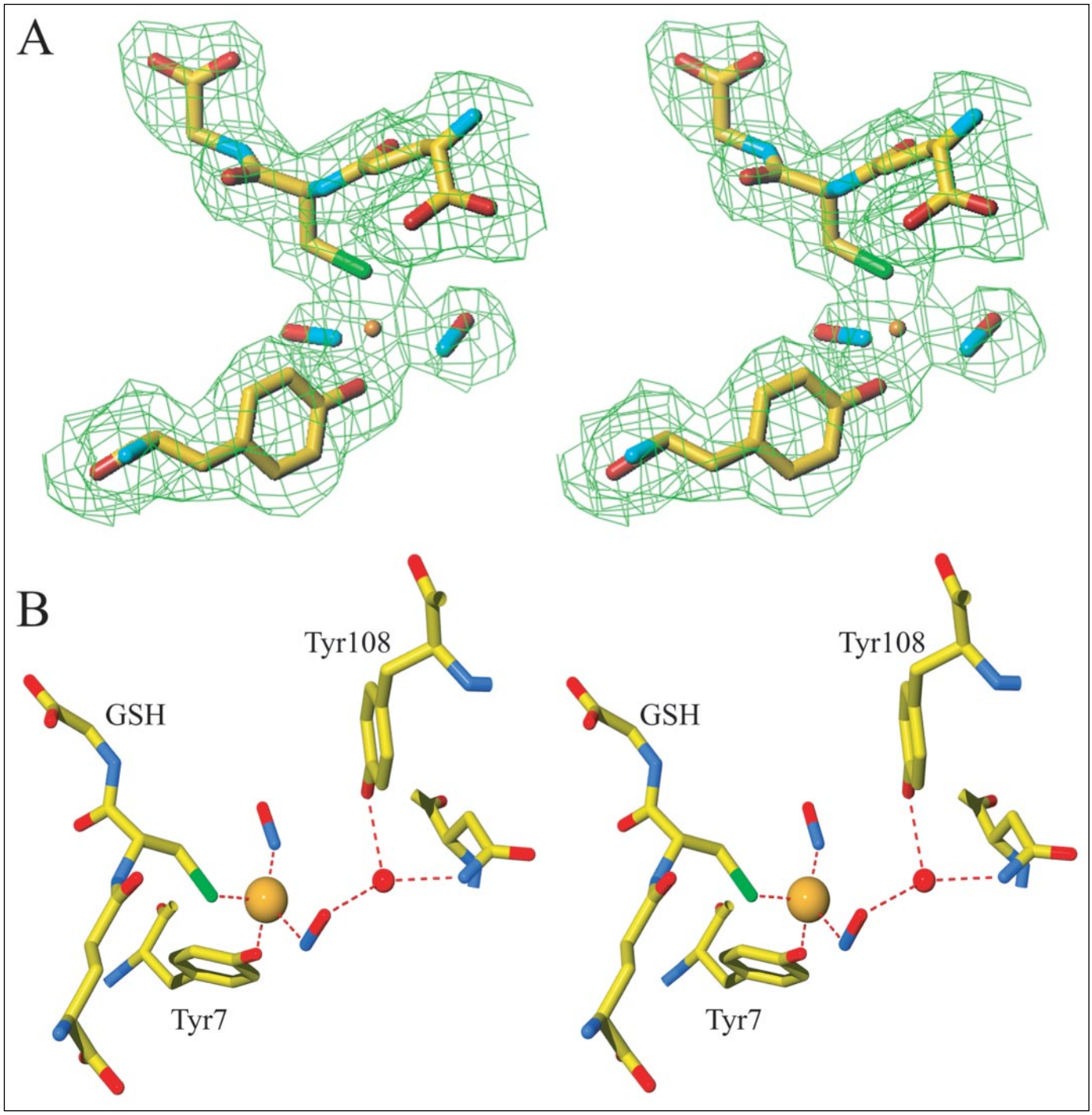

FIGURE 1. **Crystal structure of the GST P1-1 DNDGIC complex.** *A*, stereo diagram of the final $2F_o - F_c$ electron density map of the DNGIC complex at 2.1 Å of resolution centered about the active site. The DNGIC ligand, GSH, and Tyr-7 were omitted from the final calculation, and the map is contoured at 0.75σ. *B*, stereo diagram showing the coordination geometry of the active site.

and GST mutant enzymes were purified by affinity chromatography on immobilized glutathione (36). After affinity purification, the native and the mutant enzymes (Y7F, Y7H, and Y7C) were homogeneous as judged by SDS-PAGE (37). Protein concentration was determined by the method of Lowry *et al.* (38).

Kinetic Studies—The enzymatic activities were determined spectrophotometrically at 25 °C with CDNB as cosubstrate following the product formation at 340 nm, $\epsilon = 9600\ \text{M}^{-1}\ \text{cm}^{-1}$ (39). Spectrophotometric measurements were performed in a double beam Uvicon 940 spectrophotometer (Kontron Instruments) equipped with a thermostatted cuvette compartment. Initial rates were measured at 0.1-s intervals for a total period of 12 s after a lag time of 5 s. Enzymatic rates were corrected for the spontaneous reaction.

Apparent kinetic parameters, k_{cat}, K_m^{CDNB} were determined in 0.1 M potassium phosphate buffer, pH 6.5, and 0.1 mM EDTA, containing fixed concentrations of GSH (10 mM) and variable concentrations of CDNB (0.1–2 mM). The collected data were fitted to the Michaelis-Menten equation by non-linear regression analysis using the GraphPad Prism (GraphPad Software, San Diego, CA). The apparent K_m^{GSH} was also determined at a fixed CDNB concentration (1 mM) and variable

TABLE TWO

Steady-state kinetic properties of wild type and Tyr7 mutant enzymes

See "Experimental Procedures" for experimental conditions.

Enzyme	K_m^{GSH}	K_m^{CDNB}	k_{cat}	K_i^{DNDGIC}	pK_a
	mM	mM	s^{-1}	M	
WT	0.15 ± 0.04	1.2 ± 0.1	38 ± 2	$<1.5 \times 10^{-9}$	6.2
Y7F	0.16 ± 0.03	1.8 ± 0.1	0.13 ± 0.05	0.94×10^{-6}	8.14
Y7H	0.35 ± 0.08	1.24 ± 0.12	0.08 ± 0.01	7.44×10^{-7}	8.46
Y7C	0.64 ± 0.14	1.11 ± 0.02	0.73 ± 0.12	1.33×10^{-6}	7.74

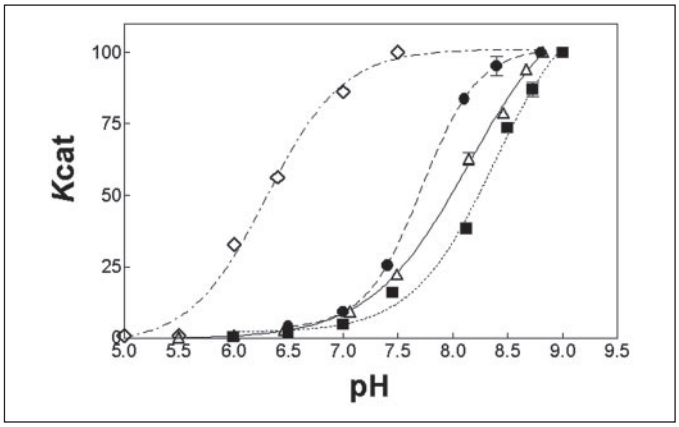

FIGURE 2. **Dependence of k_{cat} on pH.** The experimental values of k_{cat} were normalized for a useful comparison among the different mutant enzymes. The true pK_a values are reported in TABLE TWO. The experimental values refer to Y7H (■), Y7C (●), Y7F (△), and wild type (◇), respectively

GSH concentrations (from 0.02–10 mM). Kinetic parameters reported in this paper represent the mean of at least three different experimental data sets.

Cell Growth and NO Treatment of Intact Cells—Single colonies of freshly plated *E. coli* strain TOP 10 harboring plasmid pGST-1 or pGST-F7 were used to inoculate 25 ml of overnight cultures. These cultures were diluted 1:100 into Luria-Bertani medium containing 100 μg/ml ampicillin and 50 μg/ml streptomycin sulfate, grown at 37 °C to an A_{600} value of 0.5, and induced by the addition of 0.5 mM isopropyl β-D-thiogalactoside. Cells (1 liter) were grown at 37 °C for 4 h, divided in 4 aliquots (0.25 liter each), and treated as follows. (*a*) two aliquots were incubated with either 2 mM GSNO or 50 μM $FeSO_4$, one aliquot was incubated with 2 mM GSNO and 50 μM $FeSO_4$, and the last aliquot was used as the control. All the aliquots were incubated under the same conditions, at 37 °C for 15 min. (*b*) Another experimental set was established to monitor the time course of DNDGIC complex formation in which two aliquots were incubated with either 2 mM GSNO alone or 2 mM GSNO plus 50 μM $FeSO_4$ at different times (5, 15, 30, 60 min).

At the end of the incubation cells of different aliquots were harvested by centrifugation for 15 min at 7000 rpm, washed with 10 mM phosphate buffer, pH 7.0, containing 0.1 mM EDTA, and after centrifugation resuspended in a suitable volume of 10 mM phosphate buffer, pH 7.0, for electron paramagnetic resonance (EPR) analysis. The same cells were also lysed by sonication, and cell membranes were removed by centrifugation at 14,000 rpm for 10 min, and the resulting supernatant was tested for GST activity assay, protein concentration, and further EPR analysis. A similar set of experiments was also carried out using 0.5 mM DEANO (final concentration) as the NO donor instead of GSNO. We used the concentration of 2 mM GSNO throughout this work, which is the same reported previously for the DNDGIC synthesis *in vitro* (9). However, we have also exposed *E. coli* cells to different concentrations of GSNO (in a range between 0.5 and 10 mM) and obtained quite similar results to those shown in Figs. 3 and 4. As an example, after 15 min of exposure to 0.5 mM GSNO or DEANO, the GST inactivation was about 20% (despite 35% with 2 mM GSNO), whereas the EPR signal was only slightly decreased in comparison with that shown in Fig. 3*Ba* (2 mM GSNO exposure). *E. coli* cell exposure to 10 mM GSNO (a sledge hammer) only reduces GST activity 40%. To check if 2 mM GSNO concentration could inhibit cell growth, we followed bacterial growth of cells exposed to 2 mM GSNO for 24 h at 600 nm, and we found no significant difference with *E. coli* untreated cells under the same conditions (data not shown).

EPR Detection of Dinitrosyl Diglutathionyl Iron Complex—EPR spectra were recorded using 80-μl samples in flat glass capillaries (inner cross-section 5 × 0.3 mm) to optimize instrument sensitivity as previously described (40). All measurements were made at room temperature with an ESP300 X-band instrument (Bruker, Karlsruhe, Germany) equipped with a high sensitivity TM_{110}-mode cavity. Spectra were measured over a 200 G range using 20 milliwatt power, 2.0 G modulation, and a scan time of 42 s; typically 4–16 single scans were accumulated to improve the signal-to-noise ratio. High resolution spectra were recorded with 0.1-G modulation and 2 milliwatts of power. Quantitation of DNDGIC was done by incubating GSH (20 mM) and GSNO (2 mM) with variable amounts of ferrous ions (from 2 to 20 μM) under anaerobic conditions in 0.1 M potassium phosphate buffer, pH 7.4.

RESULTS

Human GST P1-1 Binds the Dinitrosyl Diglutathionyl Iron Complex at the Active Site through Tyr-7—Overall, the crystal structures of the wild-type enzyme with either GSH or the DNDGIC complex bound are very similar. Superposition of the α-carbon atoms of the GSTP1-1-DNGIC structure and the wild-type structure (5GSS) yielded a root mean square deviation of 0.27 Å for the 416 residues included in the calculation, indicating the structures are virtually identical. There are some significant, albeit small, movements of atoms close to the DNGIC ligand with some backbone atoms of the GSH molecule having moved up to 0.7 Å, the hydroxyl group of Tyr-108 moved 0.4 Å, and Phe-8 moved 0.7 Å. The most important change is that in the complex Tyr-7 binds to the iron atom through its phenolate group and in doing so displaces one of the GSH ligands (Fig. 1 and Scheme 1). The remaining iron-bound GSH ligand binds in the G-site in an almost identical manner to that observed in the structure of the GSH complex of human GST P1-1 (26). The iron atom is coordinated in a distorted tetrahedral geometry with angles between the four iron ligands (Tyr-7, GSH, and the two nitroso groups) of between 101° and 118°. Other notable interactions include Tyr-108, which forms a water-mediated hydrogen bond to the oxygen of one of the nitroso groups and a water-mediated contact between one of the nitroso groups and Asn-204.

To confirm the importance of Tyr-7 in the coordination of the iron atom of DNGIC, this residue was mutated by site-directed mutagenesis into Phe, His, or Cys, and the corresponding mutants were expressed in *E. coli*. The first mutant (Y7F) was already produced and characterized

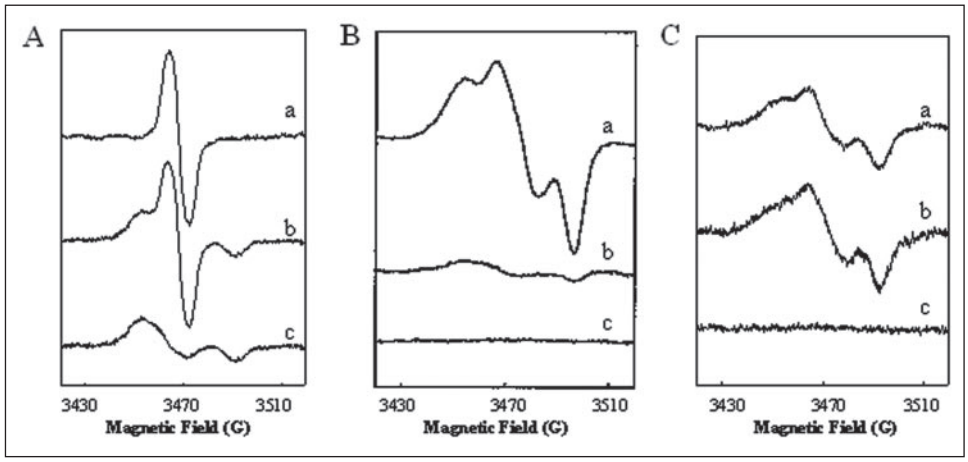

FIGURE 3. **EPR spectra.** *A*, spectra of DNDGIC free complex (*a*), Y7F mutant enzyme incubated with 5-fold excess of DNDGIC (*b*), difference spectrum, obtained by subtraction of *a* from *b*, which shows the DNDGIC bound to the mutant enzyme (minor form) (*c*). *B*, spectra of intact *E. coli* cells after 15 min of exposure to 2 mM GSNO (*a*), exposed to 2 mM GSNO and lacking the expression vector for GST P1-1 (*b*), *E. coli* cells before GSNO treatment (control) (*c*). *C*, spectra of *E. coli* extracts, (*a*) purified GST P1-1 incubated with DNDGIC, (*b*) cytosolic fraction of *E. coli* exposed to 2 mM GSNO, and (*c*) cytosolic fraction of *E. coli* exposed to 2 mM GSNO and after incubation with 10 mM KCN.

(42), whereas the other two mutants (Y7H and Y7C) were prepared and used for the first time in this study. All three mutants were easily purified from *E. coli* cells by affinity chromatography to homogeneity. The specific activity of all three Tyr-7 mutant enzymes is similar (0.2–0.4 units/mg) and very low compared with the value found in the wild-type (WT) enzyme (100 units/mg). Further investigation of the kinetic properties of these mutant enzymes compared with WT shows this low activity is a direct effect of the mutation. The results indicate that replacement of Tyr-7 with phenylalanine, cysteine, or histidine did not affect the K_m values for both substrates (GSH and CDNB) (unchanged K_m values) but dramatically reduced the k_{cat} value as compared with WT (TABLE TWO). Studies of the k_{cat} dependence on pH in the range 5.0–9.0 yielded pK_a values about 2 units higher than WT (TABLE TWO and Fig. 2). Because this pK_a has been related to the deprotonation of GSH bound into the active site (GSH-enzyme) (41) it is apparent that Tyr-7 influences greatly the acid-base equilibrium of the ternary complex (GSH-enzyme-cosubstrate), and its presence is crucial for catalysis but not for binding, as suggested by others (42).

We have previously suggested that the DNDGIC complex acts as a competitive inhibitor for the G-site of GST P1-1, and we have determined a K_i^{DNDGIC} for all these mutants (TABLE TWO). These K_i^{DNDGIC} values exhibited by all the mutant enzymes are lowered by about 3 orders of magnitude in comparison with WT. On the basis of these findings we carried out EPR experiments at room temperature on the interaction between the purified Y7F mutant enzyme and the DNDGIC complex (at different protein/complex ratios) and observed only a small fraction of the complex in a bound form, whereas the major fraction was free (Fig. 3*A*). These data, obtained from purified enzyme, indicate that removal of hydroxyl group of Tyr-7 in the enzyme active site markedly lowers the strong interaction between GST P1-1 and the complex, and neither His-7 nor Cys-7 residues were able to act as surrogates for the function of Tyr-7 (similar results by EPR and enzymatic activity assays were also obtained for the His and Cys mutant enzymes and are not shown).

GST P1-1 Is Inhibited by NO inside the Cell—We have tested the effect of NO in a simple cellular model by exposing TOP10 *E. coli* cells, overexpressing human GST P1-1, to 2 mM nitrosoglutathione for 15 min. EPR spectroscopic analysis of the intact cells showed a characteristic signal of a protein-bound dinitrosyl dithiol iron complex (Fig. 3*Ba*), and a GST assay of the same cell extracts indicated a 35% decrease of enzymatic activity compared with both the *E. coli* cells alone and the *E. coli* cells treated with $FeSO_4$ only (Fig. 4). Simultaneous exposure of the cells to both GSNO and ferrous ions did not increase the extent of the inactivation (Fig. 4) nor the intensity of EPR signal (data not shown).

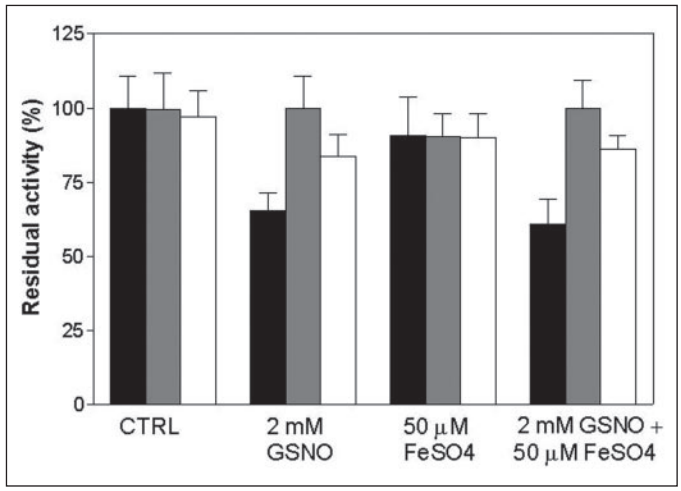

FIGURE 4. **GST specific activity in *E. coli* cells upon exposure to NO and/or iron before (*black*) and after cysteine (*white*) and cyanide (*gray*) treatment.** The experimental values of specific activity, expressed in μmol of product/min, were normalized for those of the untreated cells.

On the other hand, the addition of cysteine or potassium cyanide to the same *E. coli* extracts eliminated the signal (Fig. 3*Cc*) and recovered the original GST activity (Fig. 4), indicating that no covalent modification or irreversible inactivation has occurred. As a control, we exposed the same *E. coli* strain, lacking the expression vector for GST, to 2 mM GSNO for 15 min and carried out EPR spectroscopic analysis of both intact cells and extracts; the results showed in the intact cells the presence of a modest signal corresponding to a protein-bound dinitrosyl dithiol iron complex (Fig. 3*Bb*) that subsequently disappeared in the same extracts. The same small signal was observed when one *E. coli* strain expressing the Y7F mutant was used (data not shown). Taken together, these results suggest that the bacterial cells, in response to NO treatment, are able to form the characteristic DNDGIC complex using intracellular iron and thiol (likely GSH). This complex once formed may be trapped in a transient way by unknown proteins or much better stabilized by human GST P1-1 when present but not by its Y7F mutant.

The Lifetime of the Dinitrosyl Diglutathionyl Iron Complex Bound to GST P1-1 Is Dependent on Iron Availability in the Cell—We observed the lifetime of the DNDGIC complex bound to the protein by exposing *E. coli* cells to GSNO for different times at each time point, carrying out EPR spectra of intact cells and monitoring GST activity in the same cell extracts. It appears that the maximum extent of enzymatic inactivation (about 40%) can be reached after 5 min of GSNO exposure followed by

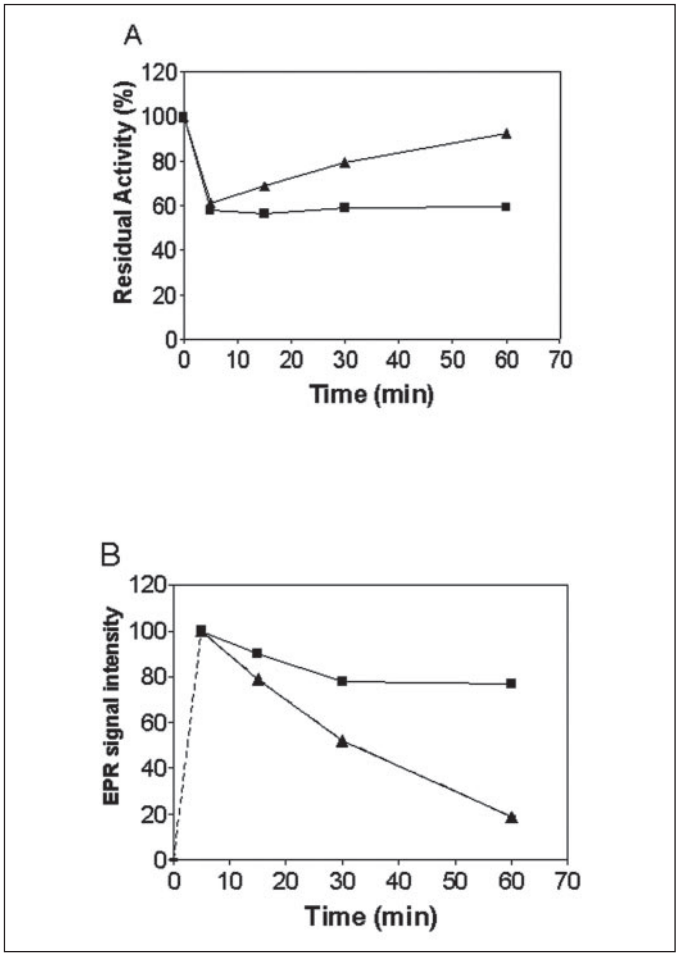

FIGURE 5. **Time course of DNGIC complex bound to GST P1-1 in *E. coli* cells after NO treatment.** *A*, GST activity as assayed in the *E. coli* cytosolic extract. *B*, EPR signal measured in intact *E. coli* cells after treatment with 2 mM GSNO (▲) or 2 mM GSNO plus $FeSO_4$ 50 μM (■). The *dashed line* indicates the unknown kinetics of DNDGIC formation.

a recovery that tends to be completed within 1 h (Fig. 5*A*). Concomitant with the activity recovery there is a loss of EPR signal down to about 20% of the original intensity within the same time (Fig. 5*B*). This indicates that inside the cellular milieu, formation and binding of this complex can be reversible, even in the presence of an overexpressed protein that has an extraordinary affinity for it (9). When this experiment was repeated in the presence of both GSNO and ferrous ions, the enzymatic inactivation and the EPR signal intensity remained constant over time (Figs. 5, *A* and *B*). Therefore, when iron is supplied from outside the cell the DNGIC-GST P1-1 complex remains stable.

DISCUSSION

In this paper we provide compelling evidence that GSTs can bind NO donors (such as DNDGIC) at the active site using as a fourth ligand, the catalytic Tyr (Tyr-7 in GST P1-1), thus confirming the hypotheses proposed in previous papers (9–11). The crystal structure provides the first structural view of the DNDGIC complex and first view of it bound to a protein and, therefore, may be of value for other studies concerning these biological complexes. The structure of this NO donor bound at the active site shows that 1) one GSH ligand is displaced and that the remaining GSH ligand of the complex binds in the G-site in an almost identical manner to that of the structure of GSH bound to GST; 2) iron binds in the complex in a distorted tetrahedral geometry with angles between the four iron ligands, Tyr-7, GSH, and the two nitroso groups, between 101° and 118°; 3) the protein side chain that is involved in covalent attachment with the complex is Tyr-7; 4) that other significant residues involved in the binding of the complex are Tyr-108 and Asn-204, both of which form water-mediated hydrogen bonds with the oxygen of one of the nitroso groups. Site-directed mutagenesis studies of Tyr-7 are consistent with the crystallographic data. Change of this residue is detrimental for the binding of DNDGIC at the active site, as demonstrated by the strong decrease of K_i^{DNDGIC} (TABLE TWO) and by EPR spectra, which show that the equilibrium between the bound and free form of DNDGIC complex is shifted toward the free form in all Tyr mutants (Fig. 3*A*). In previous studies (42) the importance of Tyr-7 in catalysis was emphasized but not its role in GSH binding (because there were no changes in K_m or K_D values between WT and Tyr-7 mutant enzymes). The results reported here suggest a specific and new function of Tyr-7 in stabilizing DNDGIC in the active site through a covalent binding to the iron atom.

In studying the DNDGIC formation inside the cell we have used *E. coli* cells because they possess a unique class of GST (GST B1-1) unable to bind this complex (10) and with no detectable CDNB activity in the cytosolic extracts. Therefore, the GST activity (4 units/mg) measured in the extracts of *E. coli* cells grown at 37 °C and 4 h after isopropyl 1-thio-β-D-galactopyranoside induction (see "Experimental Procedures") account entirely for the human recombinant GST P1-1 activity. Experiments with *E. coli* cells overexpressing human GST P1-1 demonstrated for the first time the *in vivo* formation of the DNDGIC complex upon exposure to 2 mM GSNO (Fig. 3*Ba*) (see "Experimental Procedures" for the range of GSNO concentrations used). The partial but significant inhibition of GST P1-1 in the same cell extracts (Fig. 4) suggests that the DNDGIC complex is tightly bound to the GST P1-1 active site, and only cysteine or, more efficiently, potassium cyanide (in large excess with respect to the concentration of the protein bound DNDGIC complex) is able to abolish this strong interaction and restore the enzymatic activity (Fig. 4). We have previously shown that the *in vitro* formation of the DNDGIC is independent of the presence of GST P1-1 (*i.e.* there is no catalytic effect by GST) (9), and this is also the case when DNDGIC synthesis occurs in bacteria upon exposure to NO donors. Indeed, Fig. 3*Bb* shows a faint EPR signal of such a bound complex also in the absence of GST P1-1. The presence of the overexpressing GST P1-1 in bacteria is crucial to stabilize this complex; in fact, free DNDGIC has a very short half-life in solution and is never observed in the cells. Also, the partial inactivation of GST P1-1 observed in *E. coli* extracts can be explained on the basis of previous *in vitro* experiments of GST P1-1 inhibition (9) and present structural findings. We have previously reported that DNDGIC binding to GST P1-1 exhibited negative cooperativity so that only one active site in the dimer is occupied by ligand (9). The GST P1-1-DNDGIC complex crystallizes with one dimer, and thus, two active sites per asymmetric unit in the crystal. The occupancy of the DNDGIC ligand in each site is ~0.5, which is consistent with the scenario that the ligand binds to only one site in solution, but the complex crystallizes so that the GST dimer packs into the asymmetric unit in the two possible orientations so that each active site appears half occupied.

We have already shown that GSNO causes in the absence of GSH *S*-nitrosylation of both the Cys-47 and Cys-101 residues of GST P1-1, whereas in the presence of GSH and traces of ferrous ions there is always formation of DNDGIC, which binds to the active site with extraordinary affinity by competitive inhibition with respect to GSH. Because bacterial cells contain iron proteins and GSH (at millimolar concentrations) it is very likely that the DNDGIC complex inhibits GST P1-1 in a similar fashion also *in vivo*. The recovery of GST activity after KCN treatment

of *E. coli* extracts containing DNDGIC-GST (Fig. 4) is consistent with this suggestion. In fact, CN^- ions are able to bind ferrous ions to give the extremely stable $[Fe(CN)_6]^{-4}$ complex (9), and in this way they effectively destroy the active site-bound DNDGIC complex and restore the enzymatic activity. Another important piece of evidence comes from the heterologous expression of Y7F mutant inside the bacterial cells. EPR analysis of the intact cells after GSNO exposure showed only a modest signal of DNDGIC complex similar to that obtained in bacterial cells exposed to 2 mM GSNO and lacking the expression vector for GST P1-1 (data not shown) and no detectable GST activity, confirming the crucial importance of Tyr-7 in both the binding of DNDGIC and the catalytic role of this residue also *in vivo*. We have attempted purifying the human GST P1-1 bearing the bound complex from *E. coli* cells by affinity chromatography with GSH as ligand. Unfortunately, the high pH, pH 10.0, of the elution buffer destabilized the strong interaction between GST P1-1 and DNDGIC complex (data not shown), and we could not isolate the protein bearing the DNDGIC complex.

It has been reported previously that nitric oxide (administered to the cells as nitrosothiol) can cross the cell membrane and be regenerated as nitrosothiol inside the cell (43). This appears to have occurred in our experiments, where upon exposure to exogenous GSNO we observed a rapid formation of DNDGIC complex inside the cell. Very similar results have been obtained using DEANO as an exogenous NO donor; therefore, nitric oxide alone without the GSH moiety can enter into the *E. coli* cells. The critical events follow; that is, the recruitment of intracellular iron by nitrosylation of iron proteins (*e.g.* iron-sulfur proteins (44)) and utilization of intracellular GSH, leading to the synthesis of the DNDGIC complex *in vivo* (at micromolar concentrations as indicated by EPR spectra sensitivity). The importance of thiol (mostly GSH) in favoring this interaction between NO and iron has been pointed out (or as reductant to remove iron from proteins or as a ligand for iron coordination along with NO) (5), and as result there is always formation of DNDGIC complexes. Our studies add a significant piece of knowledge to this mechanism; this complex, with a very short life in solution, once formed may be trapped and stabilized by GST P1-1 (Fig. 3*Ba*).

Other experiments using EPR analysis and GST activity assays gave an insight into the lifetime of the DNDGIC complex when bound to GST P1-1 (Fig. 5, *A* and *B*). The strong and specific binding of DNDGIC complex to GST P1-1 is reversible and dependent on iron availability inside the cell; in fact, unless iron is supplied from outside of the cell, there is a recovery of nearly all GST activity and loss of EPR signal within 1 h (Fig. 5, *A* and *B*). This last result is surprising since results obtained previously *in vitro* show the DNDGIC complex remains stable for several hours when bound to GST proteins (9). It is possible, as suggested by others, that in bacterial cells iron-sulfur cluster proteins are used as a temporary source of iron to counteract the exogenous NO until there is activation of enzymatic systems able to destroy this DNDGIC complex and repair the proteins depleted of iron. We already know that a number of enzymes can be involved in NO metabolism, especially in bacteria, where upon exposure to high amounts of NO there is protein *S*-nitrosylation and in turn induction of genes controlling nitrosant metabolism (*e.g.* flavohemoglobin) (45). Our findings provide an additional glimpse of this event; on the basis of a high affinity of nitric oxide for iron, several iron proteins can be selected targets of nitrosylation with dangerous consequences; the GSH molecule, present at large levels (millimolar concentration), favors the rapid formation of more stable nitrosothiol species (DNDGIC complexes), which in turn are sequestered by GSTs, present in several tissues at micromolar concentrations. We have already described *in vitro* a sophisticated device based on intersubunit communication by which GSTs proteins can trap these complexes with one subunit while maintaining its well known detoxifying activity toward dangerous compounds with the other subunit (9), and we would speculate that GSTs can act in a similar way also *in vivo*. In fact, despite the exposure of *E. coli* cells to large amounts of GSNO (up to 10 mM), we have observed only a partial inhibition of the overexpressed GST P1-1 inside the cell (up to 40% inactivation), consistent with the data obtained *in vitro*. The next question to be addressed is, is there export of these complexes outside the cell or destruction inside? A previous report (5) suggests the possibility of a transporter located in the membrane that is able to extrude such complexes, and one could argue that membrane pumps (Phase 3), which promote the efflux of toxic GSH conjugates outside the cytosol, also play a role in the extrusion of these complexes. There is no evidence for this at moment; for example, a tightly regulated GSNO detoxification pathway has been reported in *E. coli* cells but not in eukaryotic cells, suggesting a possible destruction of such complexes inside the cell (45). Our experimental model (*E. coli* cells overexpressing human GST P1-1) is based on the fact that large amounts of GSNO (at least micromolar concentrations) enter the cell containing high GSH concentrations, iron, and overexpressed GST. Whether these conditions could have physiological relevance in eukaryotic cells in some instances (*e.g.* inflammatory diseases), where GSTs are expressed in higher concentration, remains to be established.

Acknowledgments—We thank Harry Tong and other BioCARS staff for help at the Advanced Photon Source.

REFERENCES

1. Stamler, J. S., Simon, D. I., Osborne, J. A., Mullins, M. E., Jaraki, O., Michel, T., Singel, D. J., and Loscalzo, J. (1992) *Proc. Natl. Acad. Sci. U. S. A.* **89,** 444–448
2. Broillet, M.-C. (1999) *Cell. Mol. Life Sci.* **55,** 1036–1042
3. D'Autréaux, B., Touati, D., Bersch, B., Latour, J., and Michaud-Soret, I., (2002) *Proc. Natl. Acad. Sci. U. S. A.* **99,** 16619–16624
4. Kim, Y. M., Chung, H. T., Simmons, R. L., and Billiar, T. R. (2000) *J. Biol. Chem.* **275,** 10954–10961
5. Watts, R. N., and Richardson, D. R. (2002) *Eur. J. Biochem.* **269,** 3383–3392
6. Cairo, G., and Pietrangelo, A. (2000) *Biochem. J.* **352,** 241–250
7. Boese, M., Mordvintcev, P. I., Vanin, A. F., Busse, R., and Mulsch, A. (1995) *J. Biol. Chem.* **272,** 29244–29249
8. Becker, K., Savvides, S. N., Keese, M., Schirmer, R. H., and Karplus, P. A. (1998) *Nat. Struct. Biol.* **5,** 267–271
9. Lo Bello, M., Nuccetelli, M., Caccuri, A. M., Stella, L., Parker, M. W., Rossjohn, J., McKinstry, W. J., Mozzi, A., Federici, G., Polizio, F., Pedersen, J. Z., and Ricci, G. (2001) *J. Biol. Chem.* **276,** 42138–42145
10. De Maria, F., Pedersen, J. Z., Caccuri, A. M., Antonini, G., Turella, P., Stella, L., Lo Bello, M., Federici, G., and Ricci, G. (2003) *J. Biol. Chem.* **278,** 42283–42293
11. Turella, P., Pedersen, J. Z., Caccuri, A. M., De Maria, F., Mastroberardino, P., Lo Bello, M., Federici, G., and Ricci, G. (2003) *J. Biol. Chem.* **278,** 42294–42299
12. Hayes, D. H., Flanagan, J. U., and Jowsey, I. R. (2005) *Annu. Rev. Pharmacol. Toxicol.* **45,** 51–88
13. Mannervik, B., Ålin, P., Guthenberg, C., Jensson, H., Tahir, M. K., Warholm, M., and Jörnvall, H. (1985) *Proc. Natl. Acad. Sci. U. S. A.* **82,** 7202–7206
14. Meyer, D. J., Coles, B., Pemble, S. E., Gilmore, K. S., Fraser, G. M., and Ketterer, B. (1991) *Biochem. J.* **274,** 409–414
15. Buetler, T. M., and Eaton, D. L. (1992) *J. Environ. Sci. Health C Environ. Carcinog. Ecotoxicol. Rev.* **10,** 181–200
16. Meyer, D. J., and Thomas, M. R. (1995) *Biochem. J.* **311,** 739–742
17. Dirr, H. W., Reinemer, P., and Huber, R. (1994) *Eur. J. Biochem.* **220,** 645–661
18. Wilce, M. C. J., and Parker, M. W. (1994) *Biochim. Biophys. Acta* **205,** 1–18
19. Rossjohn, J., McKinstry, W. J., Oakley, A. J., Verger, D., Flanagan, J., Chelvanayagam, G., Tan, K.-L., Board, P. G., and Parker M. W. (1998) *Structure* **6,** 309–322
20. Wilce, M. C. J., Board, P. G., Feil, S. C., and Parker, M. W. (1995) *EMBO J.* **14,** 2133–2143
21. Polekhina, G., Board P. G., Blackburn, A. C., and Parker, M. W. (2001) *Biochemistry* **40,** 1567–1576
22. Adler, V., Yin, Z., Fuchs, S. Y., Benezra, M., Rosario, L., Tew, K. D., Pincus, M. R., Ardana, M., Henderson, C. J., Wolf, C. R., Davis, R. J., and Ronai, Z. (1999) *EMBO J.* **18,** 1321–1334
23. Cho, S-G., Lee, Y. H., Park, H-S., Ryoo, K., Kang, K. W., Park, J., Eom, S. J., Kim, M. J.,

Chang, T. S., Choi, S. Y., Shim, J., Kim, Y., Dong, M.-S., Lee, M.-J., Kim, S. G., Ichijo, H., and Choi, E.-J. (2001) *J. Biol. Chem.* **276,** 12749–12755
24. Dulhunty, A., Gage, P., Curtis, S., Chelvanayagam, G., and Board, P. (2001) *J. Biol. Chem.* **276,** 3319–3323
25. Battistoni, A., Mazzetti, A. P., Petruzzelli, R., Muramatzu, M., Ricci, G., Federici, G., and Lo Bello, M. (1995) *Protein Expression Purif.* **6,** 579–587
26. Oakley, A. J., Lo Bello, M., Battistoni, A., Ricci, G., Rossjohn, J., Villar, H. O., and Parker, M. W. (1997) *J. Mol. Biol.* **274,** 84–100
27. Hart, T. W. (1985) *Tetrahedron Lett.* **26,** 2013–2016
28. Cavero, M., Hobbs, A., Madge, D., Motherwell, W. B., Selwood, D., and Potier, P. (2000) *Bioorg. Med. Chem. Lett.* **10,** 641–644
29. Hogg, N., Singh, R. J., and Kalyanaraman, B. (1996) *FEBS Lett.* **382,** 223–228
30. McDonald, C. C., Phillips, W., and Mower, H. F. (1965) *J. Am. Chem. Soc.* **87,** 3319–3326
31. Otwinowski, Z., and Minor, W. (1997) *Methods Enzymol.* **276,** 307–326
32. Brünger, A. T., Adams, P. D., Clore, G. M., DeLano, W. L., Gros, P., Grosse-Kunstleve, R. W., Jiang, J.-S., Kuszewski, J., Nilges, M., Pannu, N. S., Read, R. J., Rice, L. M., Simonson, T., and Warren, J. L. (1998) *Acta Crystallogr. Sect. D* **54,** 905–921
33. Roussel, A., and Cambillau, C. (1989) *Silicon Graphics Partners Directory*, pp. 72–78, Silicon Graphics, Mountain View, CA
34. Laskowski, R. A., MacArthur, M. W., Moss, D. S., and Thornton, J. M. (1993) *J. Appl. Crystallogr.* **26,** 283–291
35. Lo Bello, M., Battistoni, A., Mazzetti, A. P., Board, P. G., Muramatsu, M., Federici, G., and Ricci, G. (1995) *J. Biol. Chem.* **270,** 1249–1253
36. Simons, P. C., and Vander Jagt, D. L. (1977) *Anal. Biochem.* **82,** 334–341
37. Laemmli, U. K. (1970) *Nature* **227,** 680–685
38. Lowry, O. H., Rosebrough, N. J., Farr. A. L., and Randall, R. (1951) *J. Biol. Chem.* **193,** 265–275
39. Habig, W. H., and Jakoby, W. B. (1981) *Methods Enzymol.* **77,** 398–405
40. Pedersen, J. Z., and Cox, R. P. (1988) *J. Magn. Reson.* **77,** 369–371
41. Ji, X., Johnson, W. W., Sesay, M. A., Dickert, L., Prasad, S. M., Ammon, H. L., Armstrong, R. N., and Gilliland, G. L. (1994) *Biochemistry* **33,** 1043–1052
42. Kolm, R. H., Sroga G. E., and Mannervik B. (1992) *Biochem. J.* **285,** 537–540
43. De Groote, M. A., Granger, D., Xu, Y., Prince, R., and Fang, F. C. (1995) *Proc. Natl. Acad. Sci. U. S. A.* **14,** 6399–6403
44. Ding, H., and Demple, B. (2000) *Proc. Natl. Acad. Sci. U. S. A.* **97,** 5146–5150
45. Eu, J. P., Liu, L., Zeng, M., and Stamler, J. S. (2000) *Biochemistry* **39,** 1040–1047